Dynamic Force Spectroscopy of Conservative and Dissipative Forces in an Al-Au(111) Tip-Sample System

B. Gotsmann* and H. Fuchs

Physikalisches Institut, Universität Münster, D-48149 Münster, Germany

(Received 25 October 2000)

The conservative and dissipative interaction between an aluminum tip and a gold (111) surface were investigated using dynamic force spectroscopy in UHV. Complete force vs distance curves and friction coefficient vs distance curves were obtained quantitatively. The force curves were compared to the model by Muller, Yushenko, and Derjaguin, and long and short range interactions were subsequently quantified without fit parameters. A short range conservative interaction was separated from longer range van der Waals forces. The long range behavior of the damping coefficient obeys an inverse power law of third order.

DOI: 10.1103/PhysRevLett.86.2597 PACS numbers: 68.37.Ps, 02.60.Cb, 62.20.−x, 68.35.Gy

Many physical phenomena and material properties manifest themselves in the interaction of two bodies in close proximity. A possible experimental configuration is a sharp tip and a surface as used in scanned probe techniques such as scanning tunneling microscopy (STM) and atomic force microscopy (AFM). With these methods material properties may be probed with high spatial resolution of the surface. For example, force vs distance curves as obtained using AFM are characteristic for the tip and sample materials. In principle, force interactions of different physical origins can be separated from the total force interaction by considering their characteristic distance dependence. This, then, should allow the quantitative interpretation of the interactions.

Bimetallic tip-sample systems have been the object of careful AFM investigations [1–3] mostly using the static mode of operation [4]. Dynamic AFM, on the other hand, using the frequency modulation (FM) technique [5] has been proven to be capable of true atomic resolution of various materials [6]. The tip moves through the tip-sample potential with a given vibration amplitude, resulting in a shift of the resonance frequency that is used as a measure of the forces involved. In order to combine the high resolution imaging with the probing mechanical properties this frequency shift has to be interpreted. Consequently, schemes to calculate force curves $F(\tilde{z})$ from measured dynamic force spectroscopy data [7–9], i.e., frequency shift vs distance curves $\Delta f(d)$, or from frequency shift vs amplitude curves [10] were proposed.

Dynamic force spectroscopy (DFS) is, however, not limited to probing conservative forces. Further developments regard the energy loss through dissipation into the tip-sample contact [8,9]. The *excitation amplitude* of the cantilever provides a second channel of DFS, which allows us, for example, the determination of the distance-dependent damping coefficient [8,9].

This promising new technique has hardly been exploited yet. Here, we present a detailed analysis of DFS data taken with a defined tip-sample system: An Al-metallized AFM tip and a gold Au(111) surface under well-defined conditions. Conservative and dissipative interactions are analyzed quantitatively in terms of their long and short range behavior.

Our experiments were performed under ultrahigh vacuum (UHV) conditions ($p \leq 2 \times 10^{-10}$ mbar) using a commercial microscope (UHV-AFM/STM, Omicron Instruments). The Au(111) single crystal sample was prepared by repeated annealing and sputter cleaning. LEED and STM examinations confirmed the quality of the preparations showing the Au(111) $22 \times \sqrt{3}$ reconstruction on large atomically flat terraces. The silicon AFM tip was sputter cleaned and metallized with aluminum immediately before the experiments were done in the same UHV chamber.

As a first step, the contact potential and the tip shape were determined by measuring the effect of electrostatic forces. First the tip was approached up to a distance of a few nanometers from the surface. There the frequency shift was recorded as a function of the applied voltage at a fixed distance to the surface. The maximum of the resulting parabolic $\Delta f(V)$ curve denotes the point of compensated contact potential difference (CPD). With this reference point $\Delta f(d)$ curves were recorded with a defined effective voltage between tip and sample. Care was taken that no repulsive contact was obtained during the tip approach. After calculating a force distance curve from the DFS curve (see below), the tip shape can be determined from this $F(\tilde{z})$ by comparing with models of the electrostatic capacitance force [11]. (Here $\tilde{z}$ denotes the absolute tip-sample distance, while d is the distance of the undeflected lever; hence d can be given only as a relative displacement in a DFS curve.) We found an excellent agreement with the model for a spherical tip with a tip radius of $R = (35 \pm 5)$ nm and (21 ± 2) nm, corresponding to the data in Fig. 1 and 3, respectively. There was no distance dependence of the CPD. Subsequently, DFS curves [$\Delta f(d)$ and $A_{\text{exc}}(d)$] were taken with compensated CPD (up to ± 5 mV) in order to minimize capacitance

forces in the subsequent analysis. Finally, the probing of electrostatic forces was repeated at the end of the experiment to check for potential changes of the tip shape or CPD. At the end of the experiment we scanned the surface region in the imaging mode and found no plastic changes. Further, we confirmed that the tip-sample contact did not take place at a step of the surface.

Let us first consider conservative forces. In Fig. 1a a measured $\Delta f(d)$ curve with compensated CPD is shown. The conservative force calculated from the experimental data is displayed in Fig. 1b. The calculation was based on a numerical simulation of the equation of motion including the excitation circuit:

$$m_{\text{eff}}\ddot{z}(t) + \beta_l\dot{z}(t) + k_l z(t) - F_{ts}[d + z(t), \dot{z}(t)] = R(t)z(t - t_{\text{phase}}). \quad (1)$$

Here, z denotes the deflection of the cantilever, k_l the cantilever's spring constant, $m_{\text{eff}} = 4\pi^2 k_l/f_0^2$ the effective mass, f_0 the resonance frequency of the free lever, $\beta_l = 2\pi f_0 m_{\text{eff}}/Q$ the damping coefficient of the intrinsic cantilever damping, and Q the quality factor of the free lever. The tip-sample interaction is F_{ts}. The parameter d denotes the distance of the undeflected lever with respect to the sample surface. The gain signal of the amplitude control R was modeled by a PI controller

$$R(t) = P[A(t) - A_0] + I\int_{t'=0}^{t}[A(t') - A_0]\,dt'. \quad (2)$$

Here, A is the amplitude of the cantilever vibration, P, I, and t_{phase} are given by the experimental setup. The simulation models the experiment accurately. No limiting approximations about a harmonic motion or about the type of forces used are needed: the nonlinear problem is thus solved fully. Further, all input parameters are experimentally accessible.

A time-effective algorithm [8] is used varying F_{ts} in (1) until the simulated Δf matches the experimental data for every point d of a DFS curve (with an accuracy of 0.05 Hz and a discretion of the d axis of 24 pm). An advantage of this method is that no fit parameters describing the force curve $F(\tilde{z})$ are needed. Rather, complete $F(\tilde{z})$ curves can be determined which contain the long range attractive and the repulsive regime including the transition region between the two. An example of such a calculation is given in Fig. 1.

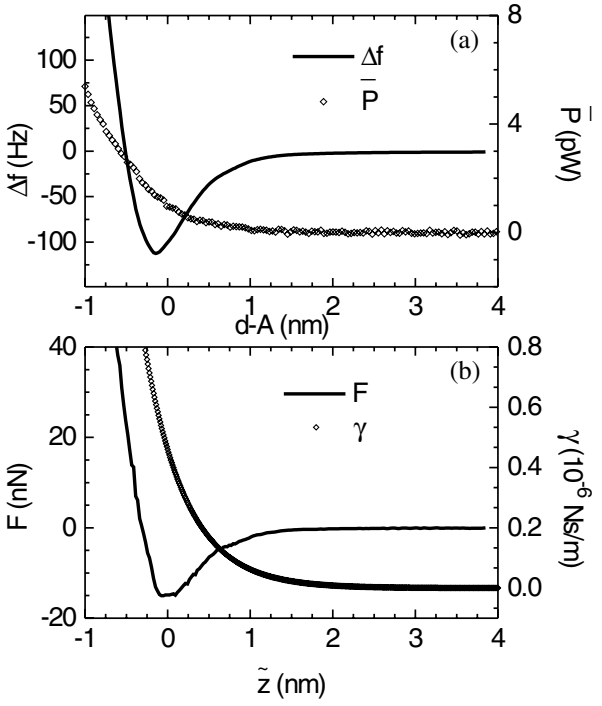

FIG. 1. Dynamic force spectroscopy of an Al tip on Au(111) (a) experimental data. The dissipation $P(d)$ was calculated from the excitation amplitude and the frequency shift using the equations given in Ref. [8]: $P = \frac{\pi k_l f(d) A^2}{Q}[\frac{R(d)}{R_0} - \frac{f(d)}{f_0}]$ (b) conservative force vs distance curve $F(\tilde{z})$ and damping coefficient vs distance curve $\gamma(\tilde{z})$ calculated numerically as in Ref. [8]. Parameters: $f_0 = 289\,210$ Hz; $A = (42,5 \pm 15)$ nm; $k_l = (50 \pm 5)$ N/m (from SEM measurements of the cantilevers dimensions); $Q = 22671$; CPD: (-496 ± 5) mV compensated.

To interpret this complete force curve it is interesting to compare the determined force interaction with a common contact model from the literature. We used the contact model by Muller, Yushenko, and Derjaguin (MYD model) [12] because it predicts complete curves and provides a more realistic physical description of the tip/sample contact than analytical models such as Hertz, DMT, JKR, etc. [13]. The model takes elasticity into consideration at every point of the curve, i.e., also in the long range attractive part, resulting in a smooth transition between the attractive and repulsive regimes. Hence adhesion as well as physically meaningful contact shapes are included.

All parameters needed for our calculation of the model are known from literature (e.g., elastic constants of tip and sample, Hamaker constant) and also the tip radius has been determined (see above)—leaving no free parameters. Hence, the model curve requires no fit to the experimental force data. Only the zero point of the reconstructed force curve (from experimental data) was chosen in accordance to the repulsive regime of the model. Now, the model itself can be put to test by comparing the reconstructed force curve with the simulated one. Such a comparison is shown in Fig. 2. There is an excellent agreement with the model for long range van der Waals forces as well as in the repulsive regime dominated by the elastic deformation of the tip and sample surfaces. Obviously, the agreement is best in the parts which can be attributed to continuum theory, on which the MYD model is based.

Interestingly, in the short range regime there is a significant difference between the model and experimental data (Fig. 2). Apparently, an additional attractive force interaction is sensed which is not accounted for in the MYD model. As the only source of adhesion the model uses the

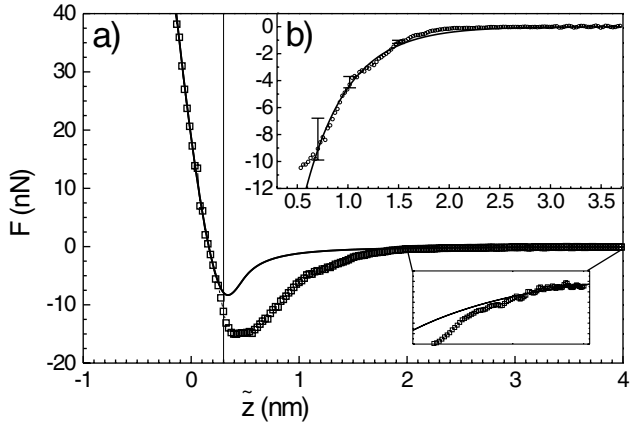

FIG. 2. (a) Reconstructed force curve from Fig. 1b together with a curve from the MYD model. (b) The difference between the two curves from (a). Parameters: Young's moduli: 42.7 GPa (Al), 62.5 GPa (Au); Poisson ratios: 0.46 (Al); 0.3625 (Au); Hamaker constant: 3.5×10^{-19} J.

van der Waals-force, which reproduces the experimental force curve well in the long range part. However, when the two surfaces reach a distance at which their electrons begin to interact, a specific electron-mediated force can be expected (see, for example, Ref. [14] and references therein for theoretical predictions, and Refs. [1–3] for experimental work), which is most likely the cause for the inconsistency. Using our data it should be possible to quantify such a specific short range interaction. For this it is essential to consider the long range van der Waals interaction which forms a background in the force interaction. This has already been pointed out by Guggisberg *et al.* [15] and Hölscher *et al.* [16] who gave careful analysis of the Si-Cu and the Si-Graphite tip-sample systems, respectively. In our case, such a separation can be made by subtracting the model curve from the reconstructed experimental force curve. This procedure is limited by the assumption that the continuum theory of van der Waals forces can be applied at tip sample distances of the order of the interatomic spacing. Further, the sample deformation is partially induced by these additional attractive forces (giving an error at distances below 0.5 nm). Finally, the choice of the zero point has a slight ambiguity of about 0.1 nm. In order to account for these aspects we chose the error bars in Fig. 2b accordingly.

Empirically, the resulting difference in the short range can be fitted well to an exponential decay curve. Although other possible distance dependencies cannot generally be excluded using these data, an exponential decay supports the speculation of an electron mediated interaction and can be expected with respect to theory [14] or other experimental data [3,15] on metal surfaces interacting via the electronic states. We find a decay length of about 0.4 nm for the given zero point as well as for a zero point shifted to the onset of repulsive forces at about $\tilde{z} = 0.35$ nm on the given scale. This decay length is surprisingly large. On the other hand, a fit of the data using a Lennard-Jones type interaction as used in Refs. [7,16] with literature values for the van der Waals force could only give a small contribution. Therefore, we believe that the observed short range force might rather be dominated by the interaction via the electronic states of tip and surface.

Let us now consider energy dissipation. The excitation amplitude can be used to determine the power loss $P(d)$ into the tip-sample interaction [8]. Assuming a viscous damping force of the form $F = -\gamma(\tilde{z})\dot{z}$ as a source of energy loss, the function $P(d)$ can be translated into $\gamma(\tilde{z})$ using numerical or semianalytical schemes [8,9]. A similar procedure as in the conservative case (combining experimental data with a simulation) leads us to a calculation of $\gamma(\tilde{z})$ from a $P(d)$ curve (as shown in Fig. 1). Such complete damping coefficient-distance curves — now accessible via DFS — invite a careful analysis. However, comparatively little is known about dissipative forces.

At distances below about 0.5 nm tip-sample contact can result in hysteresis effects in the force curve, which may dominate the dissipation. Thus, $\gamma(\tilde{z})$ is only an effective quantity in that region [9]. However, an adhesion neck appearing as a rather drastic change of the forces involved is not observed (see Ref. [3], and references therein). In the region around $\tilde{z} = 0$ a fit of an exponential decay to $\gamma(\tilde{z})$ can be used empirically to describe the qualitative behavior. Thereby we find a decay length of about 0.5 nm. However, similar to the case of conservative forces it is necessary to consider the long range behavior of the dissipation. We plotted $P(d)$ in a double logarithmic plot in Fig 3. It seems reasonably natural that a velocity dependent force as used above leads to the energy loss. Here, it is possible to use analytic formulas [8] to describe the overall behavior at distances between 1.5 and

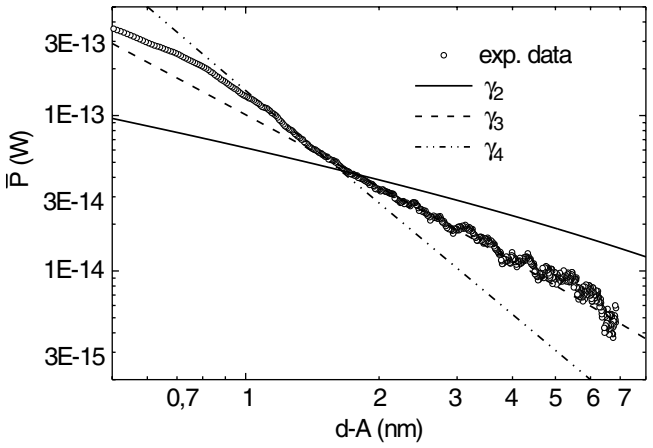

FIG. 3. Dissipation into the tip-sample interaction. Experimental data (circles) and calculated model curves (using the same parameters). The model assumes a damping coefficient which obeys an inverse power law with exponents $n = 2$ (solid line), $n = 3$ (dashed line), and $n = 4$ (dash-dotted line). Parameters: $f = 267\,220$ Hz; $A = (24 \pm 2)$ nm; $k_l = 40$ N/m; $R = (35 \pm 5)$ nm; $Q = 19\,050$; CPD compensated.

7 nm. In this way the dissipation can be attributed to a damping coefficient $\gamma(\tilde{z}) = \gamma_0 \cdot \tilde{z}^{-3}$ with a constant [17] of $\gamma_0 = (8.0^{+5.5}_{-4.5}) \times 10^{-35}$ N s m^2. The effective decay length of the short range interaction in Fig. 3 reduces after subtracting this long range background to about 0.3 nm.

The origin of the long range damping forces is unclear. The excitation or scattering of phonons and the tunneling of electrons can be excluded because of the observed long range character [18–21]. Further, the effect of electronic dissipation as proposed by Denk *et al.* [22] can be ruled out because the CPD is compensated and good conductors are used. Among other mechanisms discussed in the literature there is the van der Waals damping [19,21,23,24] (vacuum friction). A previous attempt to measure such forces was limited to larger distances, and to a less accurate method [24]. Several contradicting theories predict different magnitudes of the force (mostly much smaller than in the present experiment) and different distance dependencies [19,21,23,24]. Hence, a direct comparison of our data for the damping to an existing model from the literature cannot be given at the present stage. However, the presented data might give a quantitative framework to verify different theories.

In summary, we have presented a detailed analysis of the Al-Au(111) tip-sample interaction based on dynamic force spectroscopy data using the frequency modulation technique. The conservative and dissipative force distance relationships have been quantitatively described in their long and short range behavior.

We gratefully acknowledge financial support of the Deutsche Forschungsgemeinschaft (Fu299/8-1). We thank D. Krüger for the MYD program and C. Seidel for support with the experiments. We had fruitful discussions with I. Dorofeyev, U. D. Schwarz, and H. Hölscher.

*Electronic mail: gotsman@uni-muenster.de

[1] U. Dürig *et al.,* Phys. Rev. Lett. **65**, 349 (1990); U. Dürig *et al.,* Europhys. Lett. **23**, 147 (1993).
[2] G. Cross *et al.,* Phys. Rev. Lett. **80**, 4685 (1998).
[3] A. Schirmeisen *et al.,* Appl. Surf. Sci. **157**, 274 (2000).
[4] B. Capella and G. Dietler, Surf. Sci. Rep. **34**, 1 (1999).
[5] T. R. Albrecht *et al.,* J. Appl. Phys. **69**, 668 (1991).
[6] Proceedings of the Second International Workshop on Noncontact AFM [Appl. Surf. Sci. **140**, 243–456 (1999)].
[7] F. J. Giessibl, Phys. Rev. B **56**, 16 010 (1997).
[8] B. Gotsmann *et al.,* Phys. Rev. B **60**, 11 051 (1999).
[9] U. Dürig, New J. Phys. **2**, 5.1 (2000).
[10] H. Hölscher *et al.,* Phys. Rev. Lett. **83**, 4780 (1999).
[11] S. Hudlet *et al.,* Eur. Phys. J. **2**, 5 (1998).
[12] V. M. Muller, V. S. Yushenko, and B. V. Derjaguin, J. Colloid. Interface Sci. **77**, 91 (1980).
[13] D. Krüger, B. Anczykowski, and H. Fuchs, Ann. Phys. (Leipzig) **6**, 341 (1997).
[14] G. Bozzolo and J. Ferrante, Ultramicroscopy **42**, 55 (1992).
[15] M. Guggisberg *et al.,* Phys. Rev. B **61**, 11 151 (2000).
[16] H. Hölscher *et al.,* Phys. Rev. B **61**, 12 678 (2000).
[17] The error of the given absolute numbers is dominated by the error of k_l and A. Hence, we find an error of the F axis of about 40% and 50% for Figs. 1 and 3, respectively. This increases the uncertainty of the tip radius by this number. However, the full error is given in the case of the damping coefficient.
[18] M. Gauthier and M. Tsukada, Phys. Rev. B **60**, 11 716 (1999).
[19] J. B. Pendry, J. Phys. Condens. Matter **9**, 10 301 (1997).
[20] B. N. J. Persson, *Sliding Friction* (Springer, New York, 1998).
[21] G. V. Dedkov, Mater. Lett. **38**, 360 (1999).
[22] W. Denk and D. Pohl, Appl. Phys. Lett. **59**, 2171 (1991).
[23] A. I. Volokitin and B. N. J. Persson, J. Phys. Condens. Matter **11**, 345 (1999).
[24] I. Dorofeyev *et al.,* Phys. Rev. Lett. **83**, 2402 (1999).